

This work was written as part of one of the author's official duties as an Employee of the United States Government and is therefore a work of the United States Government. In accordance with 17 U.S.C. 105, no copyright protection is available for such works under U.S. Law.

Public Domain Mark 1.0

<https://creativecommons.org/publicdomain/mark/1.0/>

Access to this work was provided by the University of Maryland, Baltimore County (UMBC) ScholarWorks@UMBC digital repository on the Maryland Shared Open Access (MD-SOAR) platform.

**Please provide feedback**

Please support the ScholarWorks@UMBC repository by emailing [scholarworks-group@umbc.edu](mailto:scholarworks-group@umbc.edu) and telling us what having access to this work means to you and why it's important to you. Thank you.

## RESEARCH ARTICLE

10.1002/2013JD021166

## Key Points:

- Comparison of AERONET CIMEL SSA retrievals with aircraft measurements
- Assessment of mid-Atlantic aerosol via intensive study and decadal data set
- Results of DRAGON-MD/ DISCOVER-AQ Baltimore-Washington campaign are presented

## Correspondence to:

J. S. Schafer,  
joel.schafer@nasa.gov

## Citation:

Schafer, J. S., et al. (2014), Intercomparison of aerosol single-scattering albedo derived from AERONET surface radiometers and LARGE in situ aircraft profiles during the 2011 DRAGON-MD and DISCOVER-AQ experiments, *J. Geophys. Res. Atmos.*, 119, 7439–7452, doi:10.1002/2013JD021166.

Received 7 NOV 2013

Accepted 30 APR 2014

Accepted article online 6 MAY 2014

Published online 17 JUN 2014

# Intercomparison of aerosol single-scattering albedo derived from AERONET surface radiometers and LARGE in situ aircraft profiles during the 2011 DRAGON-MD and DISCOVER-AQ experiments

J. S. Schafer<sup>1,2</sup>, T. F. Eck<sup>1,3</sup>, B. N. Holben<sup>1</sup>, K. L. Thornhill<sup>4</sup>, B. E. Anderson<sup>4</sup>, A. Sinyuk<sup>1,2</sup>, D. M. Giles<sup>1,2</sup>, E. L. Winstead<sup>4</sup>, L. D. Ziemba<sup>4</sup>, A. J. Beyersdorf<sup>4</sup>, P. R. Kenny<sup>1,2</sup>, A. Smirnov<sup>1,2</sup>, and I. Slutsker<sup>1,2</sup>
<sup>1</sup>NASA Goddard Space Flight Center, Greenbelt, Maryland, USA, <sup>2</sup>Sigma Space Corporation, Lanham, Maryland, USA,

<sup>3</sup>University Space Research Association, Columbia, Maryland, USA, <sup>4</sup>NASA Langley Research Center, Hampton, Virginia, USA

**Abstract** Single-scattering albedo (SSA) retrievals obtained with CIMEL Sun-sky radiometers from the Aerosol Robotic Network (AERONET) aerosol monitoring network were used to make comparisons with simultaneous in situ sampling from aircraft profiles carried out by the NASA Langley Aerosol Group Experiment (LARGE) team in the summer of 2011 during the coincident DRAGON-MD (Distributed Regional Aerosol Gridded Observational Network-Maryland) and DISCOVER-AQ (Deriving Information on Surface conditions from Column and Vertically Resolved Observations Relevant to Air Quality) experiments. The single-scattering albedos (interpolated to 550 nm) derived from AERONET measurements for aerosol optical depth (AOD) at 440 nm  $\geq 0.4$  (mean SSA: 0.979) were on average 0.011 lower than the values derived from the LARGE profile measurements (mean SSA: 0.99). The maximum difference observed was 0.023 with all the observed differences within the combined uncertainty for the stated SSA accuracy (0.03 for AERONET; 0.02 for LARGE). Single-scattering albedo averages were also analyzed for lower aerosol loading conditions (AOD  $\geq 0.2$ ) and a dependence on aerosol optical depth was noted with significantly lower single-scattering albedos observed for lower AOD in both AERONET and LARGE data sets. Various explanations for the SSA trend were explored based on other retrieval products including volume median radius and imaginary refractive index as well as column water vapor measurements. Additionally, these SSA trends with AOD were evaluated for one of the DRAGON-MD study sites, Goddard Space Flight Center, and two other Mid-Atlantic AERONET sites over the long-term record dating to 1999.

## 1. Introduction

Unlike well-mixed, long-lived greenhouse gases, atmospheric aerosols are highly variable regionally and seasonally, and their influence on climate depends significantly on the concentration, size distribution, chemical composition and particle structure, absorption, and vertical distribution [Hansen et al., 2013]. Single-scattering albedo (SSA), the ratio of scattered to total attenuated incident sunlight, is a vital property for assessing the radiative effect of atmospheric aerosols on global climate [Haywood and Shine, 1995]. As such, this absorption parameter is a key data product of the Aerosol Robotic Network (AERONET) [Holben et al., 1998; Dubovik et al., 2002], and knowledge of the accuracy of this retrieved parameter is of critical importance to the scientific record.

A number of comparisons have been made between column-effective single-scattering albedo derived from AERONET sky-radiance measurements and SSA determined from in situ measurements taken at ground-level and in aircraft during vertical profiles over CIMEL Sun-sky radiometer sites. These include both cases of coincident measurements and those based on averaged values during extended campaign intervals [Leahy et al., 2007; Johnson et al., 2009; Schmid et al., 2006; Schafer et al., 2008; Chaudhry et al., 2007; Lee et al., 2007]. These studies have been carried out for a range of different aerosol types including biomass burning, urban pollution, and dust, and most often the in situ SSA are determined using a combination of nephelometer (for scattering component) and filter-based light absorption instrument such as an aethalometer or particle absorption photometer (for absorption component). Such efforts implicitly face a variety of challenges when comparing a column-averaged, effective SSA retrieved from a

ground-based Sun-sky radiometer which includes ensuring a complete characterization of the aerosol layer (for aircraft-measured vertical profiles) and considerations of properly accounting for air intake losses, correcting for multiple scattering of collection filters and other instrumental issues [Bond *et al.*, 1999]. Presently, aerosol light absorption measurements have larger uncertainties than extinction or scattering measurements [Sheridan *et al.*, 2005]. Surface in situ sampling may be restricted in applicability because of potential differences between aerosol characteristics at the surface and aloft. Taubman *et al.* [2006] observed a significant decrease in SSA with altitude during aircraft profiles in the mid-Atlantic United States which they attributed to a changing scattering component (absorption was found to be relatively invariant with altitude). These comparisons can still have utility particularly for comparisons with column values using SSA averaged over longer term intervals. Single-scattering albedo retrievals from Sun-sky radiometers are contingent on having relatively stable, and cloud-free aerosol conditions for the duration of the almucantar sky radiance scan and also require suitably high aerosol loading to ensure sufficient sensitivity to absorption, which can be a significant limitation in some regions.

Despite these factors, and the fact that SSA validation is often not a primary goal for field campaigns, in situ SSAs from previous studies have generally compared favorably with AERONET retrievals to a degree consistent with the stated accuracies. For aircraft comparisons with ground-based AERONET Sun-sky radiometers at multiple sites in southern Africa during SAFARI 2000, Leahy *et al.* [2007] found a mean difference (aircraft-AERONET) of  $-0.01$  (root-mean-square: 0.03) based on nephelometer and Particle Soot/Absorption Photometer (PSAP) measurements of biomass burning aerosols (though not all comparison days exceeded the required AERONET threshold of aerosol optical depth (AOD) = 0.4). Johnson *et al.* [2009] presented results from the DABEX (Dust and Biomass Experiment) campaign demonstrating a small difference in SSA of 0.02 (0.87 (in situ) versus 0.85 (CIMEL)) for aircraft in situ measurements in the Bani-zoumbou region with an AERONET Sun-sky radiometer on a day with a smoke aerosol layer located above a low-level dust layer. Campaign average surface in situ SSA measurements from nephelometer and PSAP in Rondônia, Brazil (9 September to 14 November 2002) from Schmid *et al.* [2006] were found by Schafer *et al.* [2008] to agree well with multiyear AERONET-retrieved SSA averaged for the same calendar interval ( $0.911 \pm 0.03$  (in situ);  $0.918 \pm 0.025$  (Sun photometer)). Deriving Information on Surface conditions from Column and Vertically Resolved Observations Relevant to Air Quality (DISCOVER-AQ) enabled the collection of an uncommonly large number of systematic aircraft-based measurements from numerous sites, multiple times daily, over the course of many weeks, which were well representative of the regional summer aerosol. The present study represents the most focused effort to rigorously compare AERONET single-scattering albedo retrievals with coincident and collocated aircraft in situ SSA measurements for mid-Atlantic regional urban aerosol.

## 2. Instrumentation

The AERONET aerosol monitoring network deployed more than 40 CIMEL Sun-sky radiometers in the Baltimore-Washington, DC, region for the summer 2011 DRAGON (Distributed Regional Aerosol Gridded Observational Network) campaign. This mesoscale network was comprised of the automatic Sun/sky radiometers distributed on a roughly 10 km grid (covering an area of approximately 60 km  $\times$  120 km; average distance between sites = 9.9 km) which operated continuously for more than 2 months. The full DRAGON ground network is depicted in Figure 1; aircraft altitude profile flight sites used are shown in red.

The CIMEL automatic Sun-sky radiometers are discussed at length in Holben *et al.* [1998]. Each Sun-sky radiometer deployed was equipped with multiple narrow band-pass interference filters in the visible and near-infrared with center wavelengths at 340, 380, 440, 500, 675, 870, 940, and 1020 nm (plus 1640 nm for extended wavelength versions). The 940 nm channel is used to derive column precipitable water (centimeter). The uncertainty in measured AOD, due primarily to calibration uncertainty, is  $\sim 0.010$  to 0.021 for field instruments (which is spectrally dependent with higher errors in the UV [Eck *et al.*, 1999]). The direct Sun observations are cloud screened using the method of Smirnov *et al.* [2000], and only Level 2 AOD data were used as input to the almucantar retrievals.

In addition to the direct Sun irradiance measurements that are made with a field of view of  $1.2^\circ$ , these instruments measure the sky radiance angular distribution in four spectral bands (440, 675, 870, and 1020 nm) along the solar principal plane (i.e., at constant azimuth angle, with varied view zenith angles) up to 9 times a day and along the solar almucantar (i.e., at constant solar zenith angle, with varied view

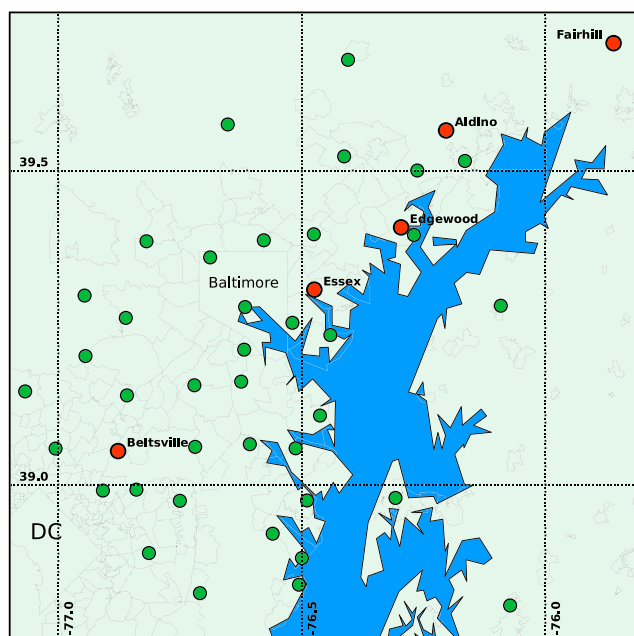


**Figure 1.** Distribution of CIMEL Sun photometer sites during DRAGON-MD (profile sites in red).

azimuth angles) up to 8 times a day (for solar zenith angle  $> 50^\circ$ ). The almucantar sky radiance measurements are taken at the following azimuth angles relative to the solar position: 3, 3.5, 4, 5, 6, 7, 8, 10, 12, 14, 16, 18, 20, 25, 30, 35, 40, 45, 50, 60, 70, 80, 90, 100, 120, 140, 160, and  $180^\circ$ . The maximum scattering angle measured ranges from approximately  $100$  to  $150^\circ$  depending on the solar zenith angle at the time of the almucantar, while the minimum scattering angle is  $3.2^\circ$ . It is these sky radiance measurements in combination with the measured spectral AOD that are used to retrieve additional column aerosol properties including volume size distribution, phase function, real and imaginary component of refractive index, effective radius, and single-scattering albedo that are routinely computed with the AERONET inversion algorithms [Dubovik and

King, 2000; Dubovik *et al.*, 2000, 2006]. Retrievals based on sky radiance measurements using this almucantar protocol have been shown to be largely insensitive to assumptions about the vertical distribution of aerosol [Torres *et al.*, 2014]. The spectral surface albedos used in the retrieval process are based on geographically and seasonally varying values estimated from the Moderate Resolution Imaging Spectroradiometer (MODIS) satellite sensor data set of midday albedos from Moody *et al.* [2005]. These spectral albedo values are averaged within a 5 km radius centered on each AERONET site for each 16 day interval. Then to compute surface albedos at a wide range of solar zenith angles (corresponding to almucantar scan times), an associated ecosystem-based bidirectional reflectance distribution function (BRDF; Li-Ross model) is utilized for ground surface type normalized by the MODIS spectral albedos for that site and date.

The retrieval parameters (e.g., SSA) are limited to those derived from almucantar procedures with low retrieval errors. The AERONET retrieval process varies the complex index of refraction, aerosol size distribution, and particle sphericity to produce the best agreement between the computed and observed radiance field from the almucantar measurement procedure as well as the AOD at four wavelengths (440, 675, 870, and 1020 nm). The root-mean-square error, weighted by measurement accuracy, is used to assess the validity of computed parameters. This residual error is required to be low ( $< 5\text{--}8\%$  depending on AOD) in order to be considered sufficient quality for the Level 2 (highest quality) AERONET data set [Dubovik *et al.*, 2000, 2006; Holben *et al.*, 2000]. This effectively requires that the almucantar be taken during cloud-free or minimally cloudy conditions, and additionally, the coincident direct Sun measurements must also have passed the standard AOD triplet variability and time series variability checks as described in Smirnov *et al.* [2000]. In order to effectively characterize the ambient aerosol, we require an almucantar to successfully acquire an empirically determined minimum number of the 28 radiance measurements from each of four predefined angular segments of the sky. A valid scan must have at least two unobstructed measurements in the range  $3.2^\circ\text{--}6^\circ$ , five in the range  $6^\circ\text{--}30^\circ$ , four in the range  $30^\circ\text{--}80^\circ$ , and three at scattering angles  $> 80^\circ$ . It is therefore possible to meet these requirements in cases with a small fraction of cloud cover. Additional checks were made to ensure that the collimator of the Sun photometer was free of any intermittent obstructions (e.g., spider web) by rejecting data when the AOD measured by the 1020 nm Si channel exceeded the AOD from the 1020 nm InGaAs channel by more than 0.05 (measurements are made with different collimators for the Si and InGaAs detectors) for the extended wavelength CIMELs (i.e., those possessing the 1640 nm channel). All the Maryland Department of Environment (MDE) profile sites were equipped with extended wavelength CIMELs.

The DRAGON-MD campaign was concurrent with the NASA sponsored DISCOVER-AQ air quality experiment which performed research flights on 14 days in July concentrating on repeated multiple daily altitudinal profile measurements of gaseous and particulate pollution over six primary Sun-sky radiometer sites. Atmospheric conditions on flight days ranged from very low AOD with low precipitable water ( $AOD_{500\text{ nm}} \sim 0.06$ ; PW:  $\sim 1.5$  cm) to extremely hazy and humid ( $AOD_{500\text{ nm}} \sim 0.9$ ; PW:  $> 4.5$  cm). In situ aerosol properties were measured on the NASA P-3B by the NASA Langley Aerosol Group Experiment (LARGE) team using a suite of instruments to characterize ambient aerosol optical and microphysical properties. Aerosol optical measurements were made with a TSI-3563 three-wavelength integrating nephelometer (450 nm, 550 nm, and 700 nm) and a three-wavelength (470 nm, 532 nm, and 660 nm) Radiance Research PSAP [Virkkula *et al.*, 2005]. We present comparisons based on coincident determinations of SSA (using three wavelengths) from AERONET CIMEL Sun-sky radiometer almucantars and column-averaged aircraft in situ observations from flight profiles at key sites.

### 3. Method

The LARGE instrument suite on the aircraft carried out measurements during profiles ranging from as low as 250 m up to greater than 5000 m at six Maryland Department of the Environment (MDE) air quality monitoring sites. On most flight days, these profiles were repeated at each MDE site 3–4 times with each profile sampling lasting about 15 min. The aircraft samples were collected during ascending or descending spirals ( $\sim 1$  km diameter) which encompassed each of the profile sites. The profiles used in this study were limited to those where sampling began below 500m and continued to greater than 1500m to provide an adequately representative column sample—the average value of the lowest sampling altitude was 367 m and the average maximum sampling altitude was 3339 m. AERONET CIMEL Sun-sky radiometers were operated at each MDE ground site (though data from the Padonia site, which had instrumental problems, was not used) and acquired aerosol optical depth (AOD) measurements at eight wavelengths every 3 min and performed up to 10 automatic almucantars per day. Additional almucantar sequences were initiated manually for cases when AERONET personnel were on site during the profile sampling event. For each profile, LARGE provided 1 s sampled values of scattering coefficient ( $\sigma_{SP}$ ) measurements at 450, 550, and 700 nm from the nephelometer and absorption coefficient ( $\sigma_{AP}$ ) measurements at 470, 532, and 660 nm from the PSAP, both from dried air samples. The small mismatch in wavelengths was corrected by linearly extrapolating the absorption coefficient values to the wavelengths of the scattering measurement which were then used to compute the SSAs at 450 nm, 550 nm, and 700 nm as defined by equation (1).

$$SSA_{(\lambda)} = \frac{\sigma_{SP}}{\sigma_{SP} + \sigma_{AP}} \quad (1)$$

At 550 nm, an additional scattering measurement at ambient relative humidity allowed for the calculation of an ambient SSA (rather than dried aerosol) that is more suitable for comparison with the SSAs derived from AERONET radiance measurements which are inherently representative of ambient atmospheric values [Ziemba *et al.*, 2013].

Ideally, for this calculation, the absorption coefficient would be measured at ambient conditions as well, but this measurement was not taken for the campaign. Absorption is somewhat less dependent on humidification than is scattering, however, so this would be a lesser effect. The CIMEL Sun-sky radiometer almucantar measurements are used to determine the column-averaged SSA at four wavelengths (440 nm, 675 nm, 870 nm, and 1020 nm), and these values were used to interpolate the SSA at the same three wavelengths at which the LARGE SSA values were calculated (450 nm, 550 nm, and 700 nm) for the comparisons. In order to produce a column SSA value to compare with AERONET, the 1 s SSA aircraft measurements were averaged for the duration of the profile sampling after weighting the values according to aerosol loading. For every profile, weighting factors for each SSA measurement were generated that corresponded to the normalized magnitude of scattering coefficient for every 1 s sample measurement, i.e., the measured SSA values were scaled proportionally to the aerosol loading at the altitude of the observation as in equation (2).

$$SSA_{(\text{weighted\_mean})} = \frac{\sum_{i=0}^N \left[ \frac{\sigma_{SP(\text{sample})}}{\sigma_{SP(\text{profile\_mean})}} * SSA_{(\text{sample})} \right]}{N} \quad (2)$$

$N$  equals the number of 1 s samples in the profile.



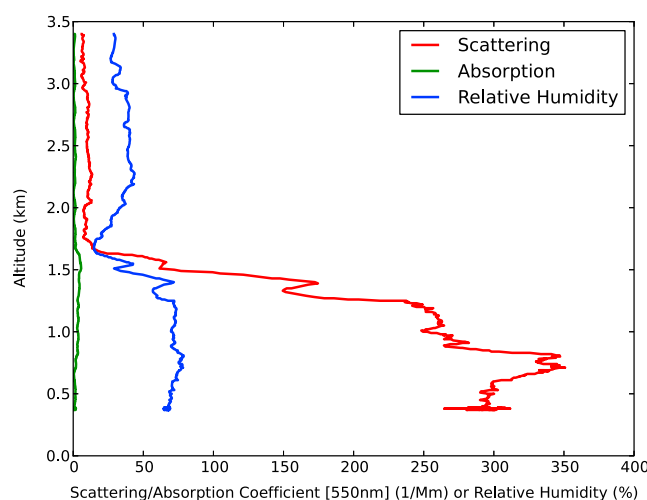


**Figure 2.** Vertical distribution of the scattering and absorption coefficient at 550 nm from LARGE profile observations (1 s samples) for the Fairhill site on 21 July at 21:38 UTC. The profile for relative humidity is also shown.

a significant decrease in aerosol loading which begins around an altitude of 1.25 km. Vertical profiles of absorption coefficient and relative humidity are also shown. Additionally, the SSA measured by LARGE at the highest altitudes (lowest aerosol loading) is substantially less than in the lower atmosphere (averaging  $0.90 \pm 0.04$  above 1.5 km and  $0.99 \pm 0.01$  below 1.5 km). For the Fairhill profile shown, the simple average would be 0.04 less than the SSA weighted by scattering magnitude. The difficulty in acquiring coincident surface and aircraft SSA measurements, even with multiple flights on 14 different days is evident in the relatively small number of time and space-matched (given the thresholds used for temporal and spatial matching here) intercomparison events. This challenge is compounded by the criteria that need to be met for AERONET-retrieved SSA values to achieve level 2 status (e.g.,  $\text{AOD} \geq 0.4$  at 440 nm with large solar zenith angle ( $\text{SZA} > 50^\circ$ ) and low residual error).

## 4. Single-Scattering Albedo Comparisons

### 4.1. Comparisons With Level 2 AERONET Data

Of the 14 LARGE flights, only six occurred on days that exceeded the 0.4 AOD threshold for even a portion of

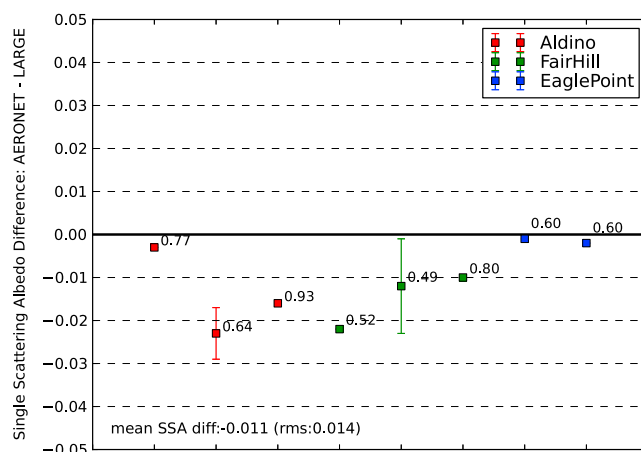


**Figure 3.** Single-scattering albedo (550nm) retrieval comparison between AERONET (Level 2 data only;  $\text{AOD}_{440 \text{ nm}} \geq 0.4$ ) and LARGE at DISCOVER-AQ profile sites (coincidence  $\pm 45$  min). Errors bars represent standard deviation for cases with multiple AERONET retrievals during match interval. The marker numbers depict the  $\text{AOD}_{440 \text{ nm}}$  observed during the measurement.

A simple average of SSAs for the full profile would give equal weight to all SSA values, including values sampled at higher altitude where the aerosol loading might be very small and thus would overrepresent the absorption features of aerosol that has negligible effect on radiation at the surface where the Sun-sky radiometer is located. Thus, we feel the most appropriate formulation of a single-column aircraft-derived SSA for comparison with AERONET-retrieved SSA is the weighted one that most strongly reflects the effect of the atmospheric aerosol extinction on radiance levels at the surface. As an example, a vertical profile of scattering coefficient (550 nm) for the Fairhill site from 21 July 2011 (Figure 2) depicts

the day, and not all these represented suitably cloud-free conditions to allow for valid almucantar observations. During the July campaign, there were 12 Level 2 AERONET SSA retrievals acquired within  $\pm 45$  min of a LARGE profile flight. Since some of these were multiple retrievals during the same profile, the total number of validation events was eight, and these occurred at three different MDE sites: Aldino, Fairhill, and Eaglepoint ( $\sim 1$  km from Edgewood MDE site). The time differences between the AERONET measurements and the central time of the LARGE profile ranged from 8 to 39 min (average time difference = 20 min). Figure 3 shows the differences in computed SSA for each of the eight validation events. The single-scattering albedos

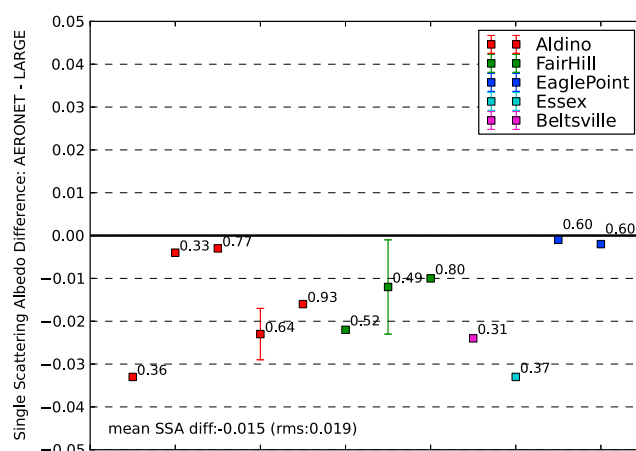


**Figure 4.** Single-scattering albedo (550 nm) retrieval comparison between AERONET (Level 1.5 data with Level 2 quality requirements but with  $AOD_{440\text{ nm}}$  threshold lowered to 0.2) and LARGE at DISCOVER-AQ profile sites (coincidence  $\pm 45$  min). Errors bars represent standard deviation for cases with multiple AERONET retrievals during match interval. The marker numbers depict the AOD observed during the measurement.

LARGE measurements (derived using absorption from dried air samples) closer to the AERONET values for cases of higher humidification.

#### 4.2. Comparisons for Lower Aerosol Optical Depth

In addition to the comparisons using LARGE and Level 2 AERONET data, we also looked at cases where all AERONET Level 2 data considerations were met except for the  $AOD_{440\text{ nm}} \geq 0.4$  constraint in order to take advantage of the cases where LARGE aircraft measurements were acquired on flight days with less aerosol loading. Generally, organic compounds are the second most abundant component of fine aerosol in the United States after sulfates [Jacobson *et al.*, 2000]. Over the course of the campaign, water-soluble organic carbon (WSOC) and sulfates were found to comprise the majority of the dry aerosol mass [Ziemba *et al.*, 2013]. Sulfates are effectively nonabsorbing [Ocko *et al.*, 2012] while some WSOC can be absorbing in the

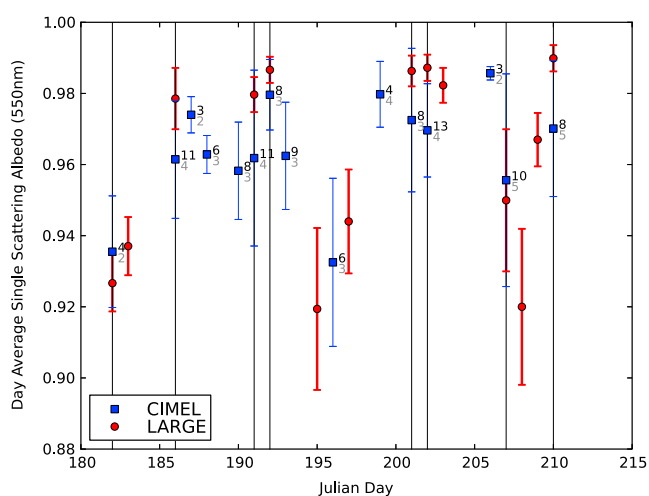


**Figure 5.** Day averages of retrieved SSA (550 nm) from DRAGON-MD MDE profile sites (blue square) and LARGE profiles (red circle) for all measurement days during the July campaign including eight coincident days (vertical lines). The number of SSA measurements in average and number of unique sites (in parentheses) are also shown. AERONET retrievals meet all Level 2 quality requirements but with  $AOD_{440\text{ nm}}$  threshold lowered to 0.2.

(550 nm) derived from AERONET measurements (mean: 0.979) were on average slightly lower than the values derived from the LARGE profile measurements (mean: 0.99) by 0.011 with a maximum difference observed of 0.023. However, all the differences are within the expected uncertainty for the stated 0.03 accuracy of the AERONET SSA measurements. The stated uncertainty for LARGE SSA measurements is 0.02. Bond *et al.* [2006] suggest that the enhancement of absorption by a nonabsorbing shell could be as much as a factor of 1.9, and more typically 1.5 depending on the relative size of the coating. An enhancement of absorption by 1.5 would reduce SSAs in the range of 0.98 by about 0.01, which might be expected to shift the SSA from the

ultraviolet and shorter blue wavelengths but are typically not strongly absorbing in the mid-visible spectrum [Chen and Bond, 2010]. Given that the dominant aerosol species are not strong absorbers, a lower AOD limit is more justifiable since relative changes in radiance are greater for a given change in SSA, and therefore, the resulting AERONET retrieval sensitivity to absorption is higher. Dubovik *et al.* [2000] computed an uncertainty of 0.03 in SSA for water-soluble aerosol for  $AOD \geq 0.2$  at 440 nm. In general, however, single-scattering albedos derived for lower AOD conditions ( $0.2 \leq AOD_{440\text{ nm}} < 0.4$ ) may have larger variability, and thus, such values are not necessarily suitable for instantaneous comparisons using individual almucantar measurements for all aerosol types. This larger variability is evident in Figure 4 which

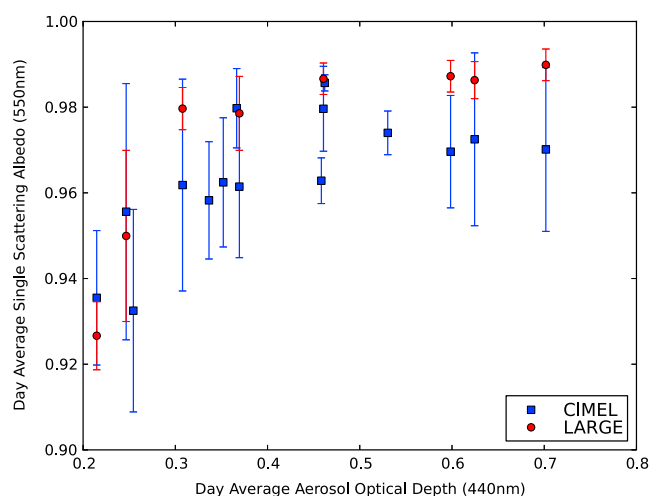


**Figure 6.** Day-averaged single-scattering albedo (550 nm) and aerosol optical depth (440 nm) for combined profile site measurements from AERONET (blue square) and LARGE (red circle) during July 2011. Aerosol optical depth represents the average of all values from almucantars used for the day.

more general comparison of aerosol absorption properties from LARGE and AERONET measurements for the study region.

In the present study, we compared the average SSA at 550 nm from the combined set of AERONET retrievals (when AOD was  $\geq 0.2$ ) acquired at all the MDE sites for each day of the campaign with the average SSA from LARGE observation for all the MDE profiles determined on the same day. Thus, a day average for the LARGE data was generally based on about 18 averages (profiles at six MDE sites repeated at least 3 times per day). For the AERONET data, the number of values included in the day average was dependent on the number of MDE sites with valid almucantars and ranged from a minimum of 3 to a maximum of 13 (average number of CIMEL retrievals/day = 7). These day-averaged SSA values at MDE sites from the LARGE profiles (14 flight days) and Sun-sky radiometer retrievals (15 days; AOD<sub>440 nm</sub>  $\geq 0.2$ ) are plotted in Figure 5. The single-scattering albedo daily averages from both LARGE and AERONET generally exhibit similar tendencies over the month of the campaign and for each of the 8 days common to both data sets

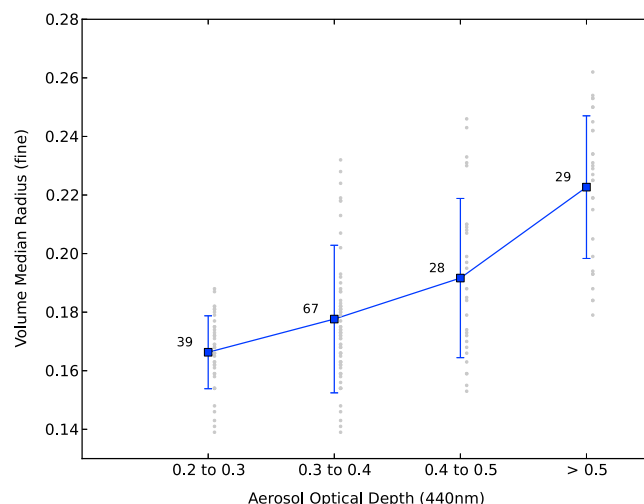


**Figure 7.** Mean volume median radius (fine mode) binned by aerosol optical depth (440 nm) for composite AERONET profile site CIMEL data during July campaign. The number of retrievals included in each bin are displayed next to the data marker.

depicts the simultaneously measured SSAs as in Figure 3, but with an allowed AOD<sub>440 nm</sub> minimum of 0.2 instead of 0.4. The comparisons are still favorable with maximum differences between in situ and surface SSA values only marginally larger than the theoretical uncertainty of 0.03 expected for weakly absorbing aerosol and a mean difference for the 12 comparison events (at five profile sites) of 0.015. When these values are taken as an ensemble, assuming that a significant part of the greater variation is due to randomly distributed measurement errors, the resulting averages of SSA and other Sun photometer retrieval products can be useful for comparison with comparable aggregate measurements from other sensors. This approach allowed for a broader and

(emphasized by vertical lines) and the difference in day SSA average for the two techniques is always within the stated accuracy of the LARGE measurement (0.02). Comparing the eight common days, the mean of the Sun-sky radiometer day averages is  $0.964(\pm 0.013)$  while the mean of the LARGE day averages is  $0.973(\pm 0.021)$  and the root-mean-square difference was 0.014. The comparable statistics for the means of all the day averages from the month of July are  $0.965(\pm 0.015)$  (AERONET) and  $0.961(\pm 0.01)$  (LARGE) though this average includes some LARGE data from days with AOD  $< 0.2$ . When the composite day-averaged SSA<sub>550 nm</sub> for the Sun-sky radiometers at the MDE sites was plotted versus the



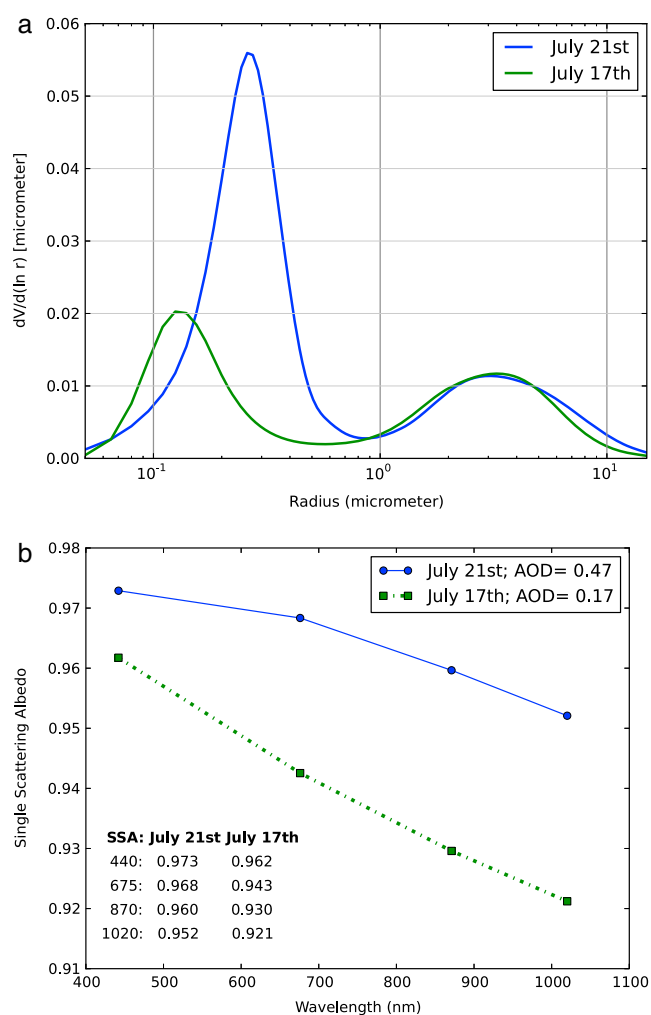


**Figure 8.** (a) Aerosol size distributions acquired at Fairhill site for a day with relatively low AOD (0.17 at 440 nm) and a day of moderate AOD (0.47). (b) Spectral single-scattering albedo modeled for two cases assuming the same complex index of refraction but different aerosol depth and aerosol size distributions (using the two size distributions shown in Figure 8a).

ity ( $RH < 40\%$ ), one at higher humidity ( $RH \sim 80\%–85\%$ ) and observed noontime hygroscopicity factors ranging from 1.28 to 1.91. On average, they estimated that the contribution of liquid-water (associated with the aerosol) to ambient visible light extinction was as much as 43% during the study interval. When the retrieved  $VMR_f$  at the AERONET MDE profile sites from the 1 month study interval is binned by AOD, the average  $VMR_f$  increases from 0.166 to 0.223  $\mu m$  from the lowest to highest AOD bin. Such a change would manifest itself as an enhancement of scattering as the fine mode peak shifted closer to the peak scattering efficiency at 550 nm, which is relevant to the SSA considered here.

To examine this effect further, aerosol size distributions acquired during the field campaign (Fairhill) were selected from a day with relatively low AOD (0.17 at 440 nm) and one of moderate AOD (0.47). The size distributions that were used for the modeling exercise are shown in Figure 8a. The standard AERONET almucantar retrieval algorithm was run for the higher AOD day to evaluate the complex refractive indices and SSA at four wavelengths (440 nm, 675 nm, 870 nm, and 1020 nm) for the observed conditions. Next, the complex refractive indices from the higher AOD day (real part = 1.46, imaginary part = 0.0057 at 440 nm) were artificially set as fixed values for the lower AOD day, and the SSAs were then modeled using the aerosol size distribution previously derived for the lower AOD day (Figure 8b). For these cases, both of which represent

day average of  $AOD_{440\text{ nm}}$  measured coincident with the almucantars, a dependence on aerosol optical depth was noted with significantly lower single-scattering albedos observed for lower aerosol optical depths (Figure 6). A similar trend in  $SSA_{550\text{ nm}}$  is also apparent when the LARGE SSA are plotted in the same manner (using column AOD from the Sun-sky radiometer measurements). This decrease in SSA for lower AOD may possibly be associated with a change in intensive properties (e.g., a shift in relative effect of scattering and absorption associated with changes in particle size distribution during low aerosol conditions), variation in the degree of particle hydration and thus scattering efficiency, as well as due to the possible increased influence of more highly absorbing aerosol versus weakly absorbing aerosol on cleaner days.

Figure 7 presents the volume median radius of the fine mode ( $VMR_f$ ) binned by  $AOD_{440\text{ nm}}$  and illustrates the monotonic increase in average particle size that we typically observe as AOD increases likely due to hygroscopic growth, coagulation processes, cloud interactions, etc. [Eck *et al.*, 2009, 2012; Schafer *et al.*, 2008; Dubovik *et al.*, 2002]. This growth in aerosol particle size is consistent with aircraft measurements with the LARGE instrument suite. Ziemba *et al.* [2013] used tandem nephelometers, one operated at low relative humid-

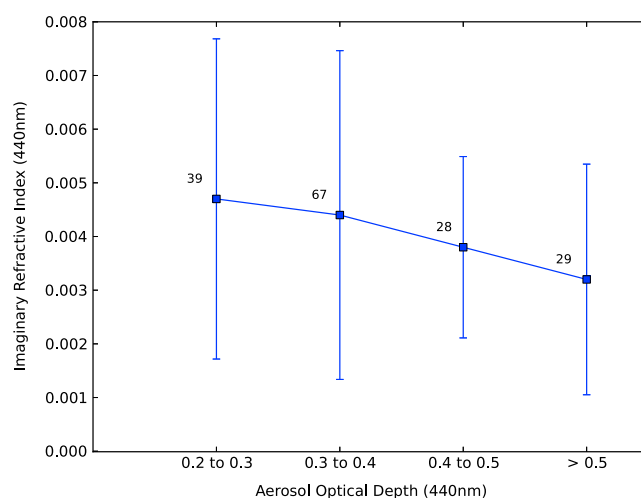


**Figure 9.** Median imaginary component of refractive index (440 nm) binned by aerosol optical depth (440 nm) for composite AERONET profile site CIMEL data during July campaign. The number of retrievals included in each bin are displayed next to the data marker.

440 nm and 0.024 at 675 nm which gives an indication of the approximate magnitude of change in SSA that might be expected to occur even when there is no compositional change in the aerosol.

Figure 9 presents the imaginary part of the refractive index binned by AOD for the composite MDE profile data set from July. This parameter is seen to decrease from 0.0047 in the lower AOD bin to 0.0032 in the highest AOD bin, which suggests that there may be a discernable change in the mean composition of the aerosol, perhaps a relatively higher contribution of more absorbing aerosol on days of low aerosol loading, e.g., carbonaceous particles of automobile and truck traffic (especially black carbon (BC) from diesel combustion) while on hazier days, hygroscopic growth, particle coagulation during aging, and potential interaction with clouds [Eck *et al.*, 2012] may proportionately increase the volume of weakly absorbing and nonabsorbing species. This is a potential explanation of the observed reduction in  $SSA_{550\text{ nm}}$  for the lower AOD days.

## 5. Analyses of Multiyear Retrieval Products for Select Sites

### 5.1. Goddard Space Flight Center

In order to expand the scope beyond the 2011 campaign, we produced a similar analysis for the Goddard Space Flight Center (GSFC) which has the longest and best-quality record since all observations are from reference Sun-sky radiometers, which have even more accurate AOD than field instruments since they are calibrated at Mauna Loa Observatory by the Langley method [Eck *et al.*, 1999]. This site is also within the DRAGON-MD study region. GSFC data from the summer months (June–August) for the interval 1999–2011 were used to produce comparable plots of retrieval products binned in five AOD bins (0.2–0.3, 0.3–0.4, 0.4–0.6, 0.6–0.8, and AOD > 0.8) and the number of almucantars in each bin ranged from 189 to 295. As observed in the combined MDE campaign data from July 2011, distinct trends as a function of AOD are seen in the long-term record (Figure 10a). The 13 years of GSFC data consistently demonstrate increasing values of average single-scattering albedo as AOD increases. This effect is most pronounced at lower AOD; however, the SSA dependence on aerosol optical depth is evident even when comparing the SSA determined for conditions greater than the standard AERONET minimum threshold for SSA retrievals from AOD of 0.4–0.6 to the highest AOD conditions (> 0.8). Similarly, AOD-binned plots are included for precipitable water, imaginary refractive index, and volume median radius (VMR). These parameters are physically linked in that larger AODs are associated with higher column water vapor (Figure 10b) due to deliquescence of aerosol particles at higher relative humidity which enhances scattering, increases particle size (and thus shifts VMR to larger values, (Figure 10d)), and reduces the imaginary part of refractive index (Figure 10c) as liquid water constitutes a greater portion of the particle. Meteorological factors also influence the PW and AOD relationship since southerly winds result in advection of warm humid air from the Gulf of Mexico in

typical aerosol size distributions observed during the summer campaign, the notable difference is the shift of the peak of the fine mode to smaller particles for the lower AOD size distribution ( $VMR_f = 0.148\text{ }\mu\text{m}$  versus  $VMR_f = 0.243\text{ }\mu\text{m}$  on the higher AOD day). Since the same real and imaginary parts of the refractive index were input for the two scenarios, the only factors causing a change in the computed SSA would be this characteristic shift in fine mode peak, and also, the lower volume concentration of the fine mode aerosol (coarse mode remained constant), which was about half the magnitude of the higher AOD day in the fine mode. For the two sample days, the net effect of these differences in the aerosol size distribution and concentration is a reduction of SSA of 0.011 at

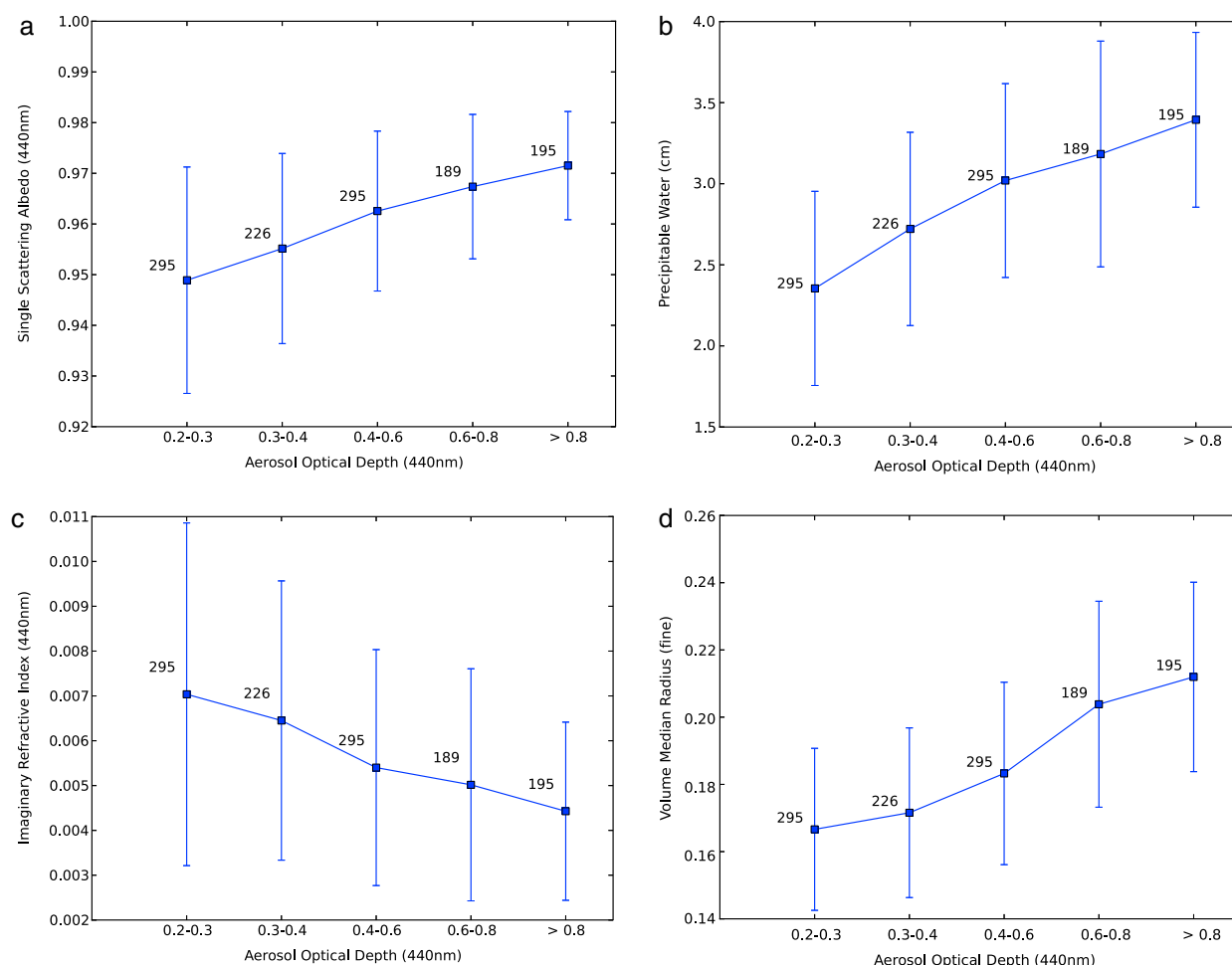


**Figure 10.** Goddard Space Flight Center retrieved parameters (1999–2011; June–August only) binned by aerosol optical depth. (a) Single-scattering albedo (440 nm), (b) aerosol optical depth (440 nm), (c) imaginary refractive index (440 nm), and (d) volume median radius of fine mode. The number of retrievals included in each bin are displayed next to the data marker.

conjunction with several sources of aerosols in the south (refineries, fossil fuel power plants, etc.) resulting in the northward advection of humidified and aged aerosols, along with aerosol precursor gases. Additionally, in general, cloud cover increases as PW increases therefore the probability of aerosol-cloud interaction likely increases, as suggested by *Eck et al.* [2012] for the GSFC site. The corresponding plots for these retrieval products binned by column water vapor are shown in Figure 11. The slope of both AOD and VMR (versus PW) increases for PW > 2.5 which might indicate relative humidity and possibly clouds have greater influence at these higher PW levels.

## 5.2. Mid-Atlantic Long-Term Site Comparison

When AOD-binned single-scattering albedo retrievals from two other long-term AERONET records (13 years of observations for each) in the mid-Atlantic region (MD Science Center: Baltimore, MD and Wallops: Eastern shore of Virginia) are compared with NASA/GSFC (Figure 12), a very similar decrease in SSA for lower aerosol optical depth conditions is observed. For moderate to high AOD, the difference in SSA for the three sites is minimal (< 0.01), while in the lowest AOD bin for which we have presented averages of retrieved SSA (AOD: 0.2–0.3), the three sites exhibit greater divergence (> 0.02 difference between Wallops and MD Science Center) (Table 1). The modest but consistent difference in SSA between sites (~0.005) for AOD > 0.3 is well within our retrieval uncertainties but is unlikely to be related to calibration differences as each average is based on measurements from Sun-sky radiometers that were recalibrated annually (often with different instruments for different years) over 13+ years and any calibration discrepancy would be expected to largely

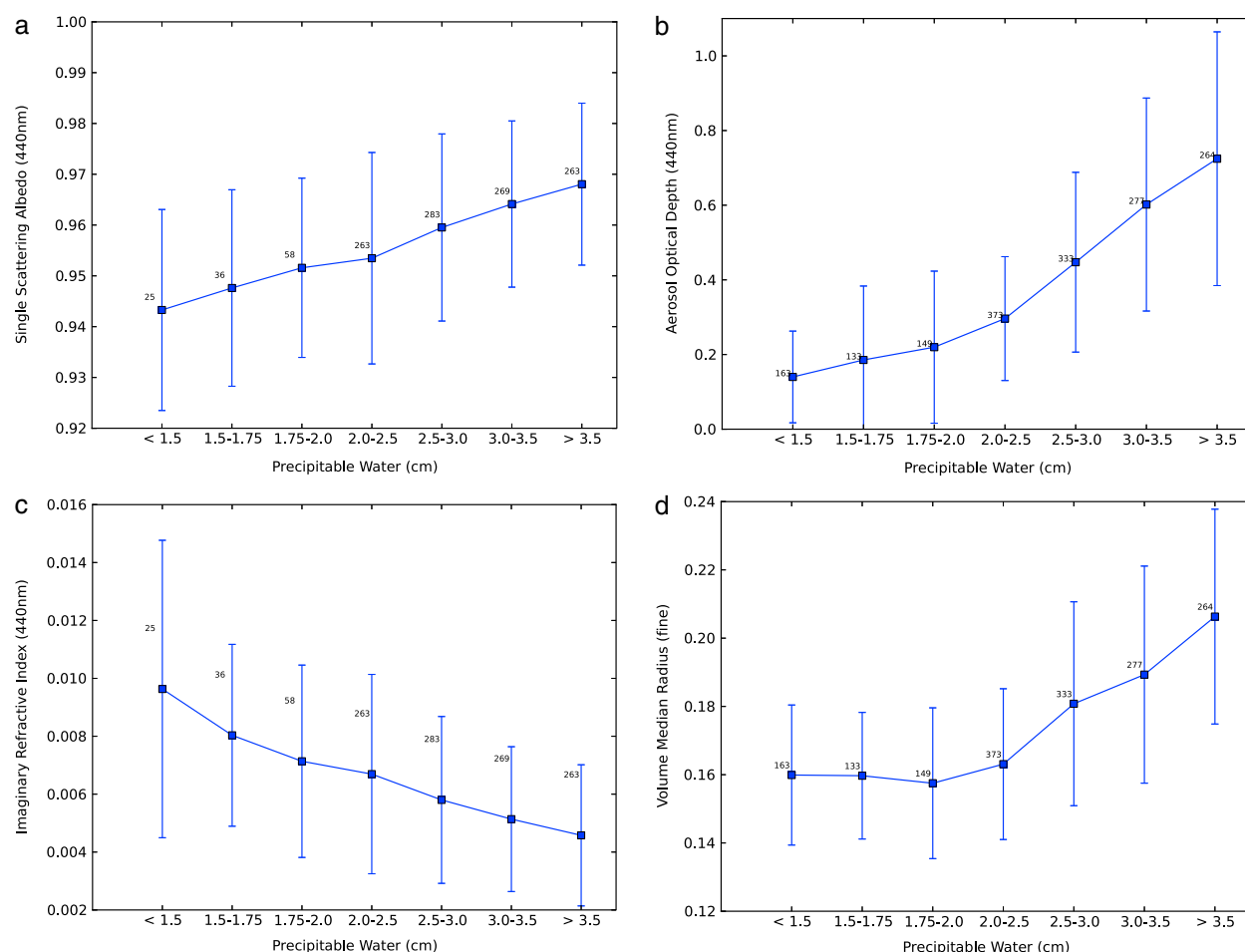


**Figure 11.** Goddard Space Flight Center retrieved parameters (1999–2011; June–August only) binned by precipitable water. (a) Single-scattering albedo (440 nm) ( $AOD \geq 0.2$ ), (b) aerosol optical depth (440 nm), (c) imaginary refractive index (440 nm) ( $AOD \geq 0.2$ ), and (d) volume median radius of fine mode. The number of retrievals included in each bin are displayed next to the data marker.

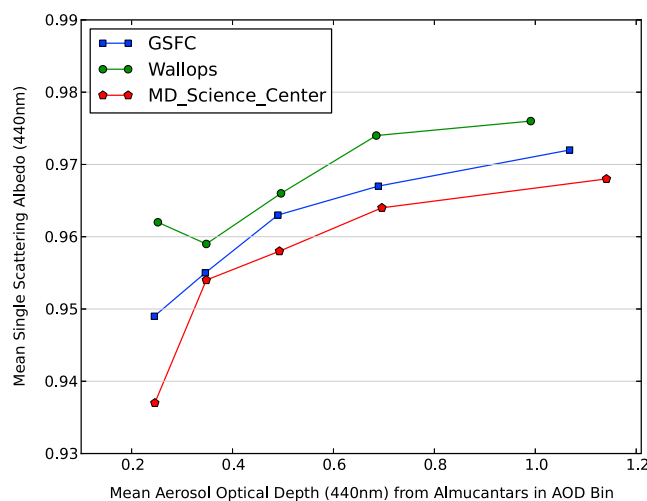


**Figure 12.** Single-scattering albedo (440 nm) binned by aerosol optical depth (440 nm) for three mid-Atlantic long-term AERONET records (1999–2011; June–August only).

average out. Variation in the accuracy of input surface albedo for each site could potentially cause small persistent differences in measured SSA, although the influence of surface albedo on the retrievals diminishes as AOD increases, and the surface albedos are estimated based on MODIS atmospherically corrected surface albedo for all three sites. Slightly less absorbing aerosol at Wallops could be explained by the fact that this is a rural, coastal site (with some influence from nonabsorbing sea-salt aerosol) while MD Science Center is situated in downtown Baltimore (with significant industrial activity and diesel-fueled ships coming into the port, with possible greater BC emissions) and so might be expected to have somewhat

**Table 1.** Statistics of Aerosol Features Binned by Aerosol Optical Depth for Three Mid-Atlantic Long-Term AERONET Records (1999–2011; June–August Only)<sup>a</sup>

Site	AOD Bin	# Retrievals	SSA <sub>440 nm</sub>	VMR <sub>fine</sub>	Imaginary Refractive Index	Angstrom Exponent
GSFC	0.1–0.2	365	NA	0.156	NA	1.79
GSFC	0.2–0.3	295	0.949	0.167	0.0070	1.88
GSFC	0.3–0.4	226	0.955	0.172	0.0065	1.91
GSFC	0.4–0.6	295	0.963	0.183	0.0054	1.89
GSFC	0.6–0.8	189	0.967	0.204	0.0050	1.80
GSFC	> 0.8	195	0.972	0.212	0.0044	1.76
Wallops	0.1–0.2	161	NA	0.163	NA	1.82
Wallops	0.2–0.3	140	0.962	0.176	0.0053	1.85
Wallops	0.3–0.4	102	0.959	0.183	0.0064	1.89
Wallops	0.4–0.6	180	0.966	0.195	0.0055	1.86
Wallops	0.6–0.8	121	0.974	0.208	0.0040	1.79
Wallops	> 0.8	120	0.976	0.215	0.0037	1.79
MD Science Center	0.1–0.2	232	NA	0.153	NA	1.79
MD Science Center	0.2–0.3	205	0.937	0.163	0.0083	1.86
MD Science Center	0.3–0.4	126	0.954	0.165	0.0060	1.93
MD Science Center	0.4–0.6	182	0.958	0.180	0.0060	1.88
MD Science Center	0.6–0.8	115	0.964	0.199	0.0054	1.81
MD Science Center	> 0.8	144	0.968	0.213	0.0049	1.75

<sup>a</sup>NA, not available.

more absorbing aerosol than GSFC, a distant suburb of Washington, DC (a nonindustrial city). The general trend in single-scattering albedo is one of decreasing values with lower aerosol optical depth for each of these mid-Atlantic locations, with the exception of a contrary increase of SSA at Wallops for the lowest AOD bin. However, this feature is consistent with the fact that aerosol at this coastal site has a larger contribution from sea-salt particles which are nonabsorbing and also highly hydrophilic. *Giles et al.* [2012] found the decade average Angstrom absorption exponent for GSFC to be  $1.1 \pm 0.2$  which is consistent with an assumption that black carbon is the primary absorbing species in this region [*Bergstrom et al.*, 2002]. If the urban MD Science Center site typically experiences aerosols with a higher black carbon content, then this might manifest as a relatively stronger decrease in SSA for lower AOD conditions. Compositional differences would have the most pronounced effect on SSA for the lowest AOD (and least humidified) scenario and the larger imaginary refractive index at this site ( $\sim 0.008$ ) relative to GSFC (0.007) in the lowest AOD bin is consistent with this hypothesis (Table 1).

## 6. Conclusions

Single-scattering albedo retrievals from the AERONET network of Sun-sky radiometers were compared with corresponding weighted averages from coincident ( $\pm 45$  min) LARGE suite of in situ instruments on aircraft altitudinal profiles for multiple collocated sites during the DRAGON-MD and DISCOVER-AQ campaigns. The mean agreement for the simultaneous comparisons meeting the AERONET minimum aerosol optical depth threshold of 0.4 (at 440 nm) was excellent (SSA difference of 0.011 at 550 nm), and all of the coincident measurement pairs were within the accuracies of the measurement techniques suggesting that good agreement may be consistently obtained between Sun-sky radiometer and in situ measurements when a careful intercomparison protocol is rigorously applied. The opportunity to expand the range of comparisons with the LARGE in situ measurements was motivation to examine cases with a lower threshold of  $\text{AOD}_{440 \text{ nm}} \geq 0.2$ . Despite relatively larger uncertainty in retrieved SSA from individual almucantars at these lower AOD levels, there can be some utility in such observations when averaged values are used and the observed aerosol is known to be weakly absorbing. For the 8 days with a suitable number of AERONET retrievals from multiple profile sites, the day averages of SSA from aircraft and Sun photometers also agreed very well (CIMEL:  $0.964(\pm 0.013)$ ; LARGE:  $0.973(\pm 0.021)$ ) although half of these days had average AOD in the 0.2 to 0.4 range. Increasing trends in SSA as AOD increased were observed for both in situ (LARGE) and column-averaged (AERONET) measurements, which were possibly due to a variety of contributing factors. The highly hydrophilic nature of mid-Atlantic urban aerosol [*Kotchenruther et al.*, 1999] results in significant particle growth by hydration which shifts the size distribution (enhancing scattering) and lowers the imaginary refractive index (with the addition of nonabsorbing liquid water), both of which can potentially increase the SSA. Additionally, aerosol growth due to coagulation and cloud processing events are also likely



correlated with aerosol concentration (and thus aerosol optical depth) and PW (related to cloud fraction), respectively, and therefore, these aerosol aging and particle modification processes also likely play a role in the observed dependence of SSA on AOD. At lower AOD (correlated with low PW), when the dominance of hygroscopic aerosol is diminished, the background industrial signal of more strongly absorbing ambient black carbon aerosol may possibly produce small but distinct regional differences in SSA, as seen in the comparison of three long-term SSA records from mid-Atlantic AERONET sites.

## Acknowledgments

The AERONET project is supported by the Radiation Sciences Program (NASA), the EOS project office (NASA), and the Joint Polar Satellite System program (NOAA). We would like to thank the summer interns who installed and maintained the 40+ CIMEL Sun photometers; Anastasia Sorokine, Chris McPartland, Christopher Blackwell, Sarah Dickerson, and Christina Justice as well as the many local elementary schools and high schools that hosted our instrumentation for several months. Additionally, we would like to recognize the contributions of Jennifer Hains, Ryan Auvil, and others at the Maryland Department of the Environment who allowed us to operate our equipment at their facilities. The data used in this paper are available at 'http://aeronet.gsfc.nasa.gov/new\_web/DRAGON-USA\_2011\_DC\_Maryland.html'

## References

- Bergstrom, R. W., P. B. Russell, and P. Hignett (2002), Wavelength dependence of the absorption of black carbon particles: Predictions and results from the TARFOX experiment and implications for the aerosol single scattering albedo, *J. Atmos. Sci.*, *59*(3), 567–577, doi:10.1175/1520-0469(2002)059<0567:WDOTAO>2.0.CO;2.
- Bond, T. C., T. L. Anderson, and D. Campbell (1999), Calibration and intercomparison of filter-based measurements of visible light absorption by aerosols, *Aerosol Sci. Technol.*, *30*(6), 562–600, doi:10.1080/027868299304435.
- Bond, T. C., G. Habib, and R. W. Bergstrom (2006), Limitations in the enhancement of visible light absorption due to mixing state, *J. Geophys. Res.*, *111*, D20211, doi:10.1029/2006JD007315.
- Chaudhry, Z., J. V. Martins, Z. Li, S.-C. Tsay, H. Chen, P. Wang, T. Wen, C. Li, and R. R. Dickerson (2007), In situ measurements of aerosol mass concentration and radiative properties in Xianghe, southeast of Beijing, *J. Geophys. Res.*, *112*, D23S90, doi:10.1029/2007JD009055.
- Chen, Y., and T. C. Bond (2010), Light absorption by organic carbon from wood combustion, *Atmos. Chem. Phys.*, *10*(4), 1773–1787, doi:10.5194/acp-10-1773-2010.
- Dubovik, O., and M. D. King (2000), A flexible inversion algorithm for retrieval of aerosol optical properties from Sun and sky radiance measurements, *J. Geophys. Res.*, *105*(D16), 20,673–20,696.
- Dubovik, O., A. Smirnov, B. N. Holben, M. D. King, Y. J. Kaufman, T. F. Eck, and I. Slutsker (2000), Accuracy assessments of aerosol optical properties retrieved from Aerosol Robotic Network (AERONET) Sun and sky radiance measurements, *J. Geophys. Res.*, *105*(D8), 9791–9806.
- Dubovik, O., B. N. Holben, T. F. Eck, A. Smirnov, Y. J. Kaufman, M. D. King, D. Tanre, and I. Slutsker (2002), Variability of absorption and optical properties of key aerosol types observed in worldwide locations, *J. Atmos. Sci.*, *59*, 590–608, doi:10.1175/1520-0469(2002)059<0590:VOAOP>2.0.CO;2.
- Dubovik, O., et al. (2006), Application of spheroid models to account for aerosol particle nonsphericity in remote sensing of desert dust, *J. Geophys. Res.*, *111*, D11208, doi:10.1029/2005JD006619.
- Eck, T. F., B. N. Holben, J. S. Reid, O. Dubovik, A. Smirnov, N. T. O'Neill, I. Slutsker, and S. Kinne (1999), Wavelength dependence of the optical depth of biomass burning, urban, and desert dust aerosols, *J. Geophys. Res.*, *104*(D24), 31,333–31,349.
- Eck, T. F., et al. (2009), Optical properties of boreal region biomass burning aerosols in central Alaska and seasonal variation of aerosol optical depth at an Arctic coastal site, *J. Geophys. Res.*, *114*, D11201, doi:10.1029/2008JD010870.
- Eck, T. F., et al. (2012), Fog- and cloud-induced aerosol modification observed by the Aerosol Robotic Network (AERONET), *J. Geophys. Res.*, *117*, D07206, doi:10.1029/2011JD016839.
- Giles, D. M., B. N. Holben, T. F. Eck, A. Sinyuk, A. Smirnov, I. Slutsker, R. R. Dickerson, A. M. Thompson, and J. S. Schafer (2012), An analysis of AERONET aerosol absorption properties and classifications representative of aerosol source regions, *J. Geophys. Res.*, *117*, D17203, doi:10.1029/2012JD018127.
- Hansen, J., P. Kharecha, and M. Sato (2013), Climate forcing growth rates: Doubling down on our Faustian bargain, *Environ. Res. Lett.*, *8*, 011006. [Available at <http://stacks.iop.org/1748-9326/8/i=1/a=011006>.]
- Haywood, J. M., and K. P. Shine (1995), The effect of anthropogenic sulfate and soot aerosol on the clear sky planetary radiation budget, *Geophys. Res. Lett.*, *22*(5), 603–606, doi:10.1029/95GL00075.
- Holben, B. N., et al. (1998), AERONET- A federated instrument network and data archive for aerosol characterization, *Remote Sens. Environ.*, *66*, 1–16, doi:10.1016/S0034-4257(98)00031-5.
- Holben, B. N., T. F. Eck, I. Slutsker, A. Smirnov, J. Schafer, D. Giles, and O. Dubovik (2006), Aeronet's Version 2.0 quality assurance criteria, *Proceedings- SPIE the International Society for Optical Engineering*, *6408*, 64080Q, *Conference on Remote Sensing of the Atmosphere and Clouds*, Goa, India, 13–16 November, doi:10.1117/12.706524.
- Jacobson, M. C., H.-C. Hansson, K. J. Noone, and R. J. Charlson (2000), Organic atmospheric aerosols: Review and state of the science, *Rev. Geophys.*, *38*(2), 267–294, doi:10.1029/1998RG000045.
- Johnson, B. T., S. Christopher, J. M. Haywood, S. R. Osborne, S. McFarlane, C. Hsu, C. Salustro, and R. Kahn (2009), Measurements of aerosol properties from aircraft, satellite and ground-based remote sensing: A case-study from the Dust and Biomass-burning Experiment (DABEX), *Q. J. R. Meteorol. Soc.*, *135*, 922–934, doi:10.1002/qj.420.
- Kotchenruther, R., P. Hobbs, and D. Hegg (1999), Humidification factors for atmospheric aerosols off the mid-Atlantic coast of the United States, *J. Geophys. Res.*, *104*, 2239–2251, doi:10.1029/98JD01751.
- Leahy, L. V., T. L. Anderson, T. F. Eck, and R. W. Bergstrom (2007), A synthesis of single scattering albedo of biomass burning aerosol over southern Africa during SAFARI 2000, *Geophys. Res. Lett.*, *34*, L12814, doi:10.1029/2007GL029697.
- Lee, K. H., Z. Li, M. S. Wong, J. Xin, Y. Wang, W.-M. Hao, and F. Zhao (2007), Aerosol single scattering albedo estimated across China from a combination of ground and satellite measurements, *J. Geophys. Res.*, *112*, D22S15, doi:10.1029/2007JD009077.
- Moody, E. G., M. D. King, S. Platnick, C. B. Schaaf, and F. Gao (2005), Spatially complete global spectral surface albedos: Value-added datasets derived from Terra MODIS land products, *IEEE Trans. Geosci. Remote Sens.*, *43*(1), 144–158, doi:10.1109/TGRS.2004.838359.
- Ocko, I. B., V. Ramaswamy, P. Ginoux, Y. Ming, and L. W. Horowitz (2012), Sensitivity of scattering and absorbing aerosol direct radiative forcing to physical climate factors, *J. Geophys. Res.*, *117*, D20203, doi:10.1029/2012JD018019.
- Schafer, J. S., T. F. Eck, B. N. Holben, P. Artaxo, and A. F. Duarte (2008), Characterization of the optical properties of atmospheric aerosols in Amazônia from long-term AERONET monitoring (1993–1995 and 1999–2006), *J. Geophys. Res.*, *113*, D04204, doi:10.1029/2007JD009319.
- Schmid, O., P. Artaxo, W. P. Arnott, D. Chand, L. V. Gatti, G. P. Frank, A. Hoffer, M. Schnaiter, and M. O. Andreae (2006), Spectral light absorption by ambient aerosols influenced by biomass burning in the Amazon Basin: Part I: Comparison and field calibration of absorption measurement techniques, *Atmos. Chem. Phys.*, *6*, 3443–3462.

- Sheridan, P. J., et al. (2005), The reno aerosol optics study: An evaluation of aerosol absorption measurement methods, *Aerosol Sci. Technol.*, 39(1), 1–16, doi:10.1080/027868290901891.
- Smirnov, A., B. N. Holben, T. F. Eck, O. Dubovik, and I. Slutsker (2000), Cloud-screening and quality control algorithms for the AERONET database, *Remote Sens. Environ.*, 73(3), 337–349.
- Torres, B., O. Dubovik, C. Toledano, A. Berjon, V. E. Cachorro, T. Lapyonok, P. Litvinov, and P. Goloub (2014), Sensitivity of aerosol retrieval to geometrical configuration of ground-based Sun/sky radiometer observations, *Atmos. Chem. Phys.*, 14, 847–875, doi:10.5194/acp-14-847-2014.
- Taubman, B. F., J. C. Hains, A. M. Thompson, L. T. Marufu, B. G. Doddridge, J. W. Stehr, C. A. Piety, and R. R. Dickerson (2006), Aircraft vertical profiles of trace gas and aerosol pollution over the mid-Atlantic United States: Statistics and meteorological cluster analysis, *J. Geophys. Res.*, 111, D10S07, doi:10.1029/2005JD006196.
- Virkkula, A., N. C. Ahlquist, D. S. Covert, P. J. Sheridan, W. P. Arnott, and J. A. Ogren (2005), A three-wavelength optical extinction cell for measuring aerosol light extinction and its application to determining light absorption coefficient, *Aerosol Sci. Technol.*, 39(1), 52–67, doi:10.1080/027868290901918.
- Ziemba, L. D., et al. (2013), Airborne observations of aerosol extinction by in situ and remote-sensing techniques: Evaluation of particle hygroscopicity, *Geophys. Res. Lett.*, 40, 417–422, doi:10.1029/2012GL054428.